

University of Nebraska - Lincoln

DigitalCommons@University of Nebraska - Lincoln

Faculty Publications, Department of Physics
and Astronomy

Research Papers in Physics and Astronomy

1-15-2021

Surface acoustic waves increase magnetic domain wall velocity

Anil Adhikari

S. Adenwalla

Follow this and additional works at: <https://digitalcommons.unl.edu/physicsfacpub>




Part of the [Physics Commons](#)

This Article is brought to you for free and open access by the Research Papers in Physics and Astronomy at DigitalCommons@University of Nebraska - Lincoln. It has been accepted for inclusion in Faculty Publications, Department of Physics and Astronomy by an authorized administrator of DigitalCommons@University of Nebraska - Lincoln.

Surface acoustic waves increase magnetic domain wall velocity


Cite as: AIP Advances **11**, 015234 (2021); <https://doi.org/10.1063/9.0000159>

Submitted: 22 October 2020 . Accepted: 04 December 2020 . Published Online: 15 January 2021

 A. Adhikari, and S. Adenwalla

COLLECTIONS

Paper published as part of the special topic on [65th Annual Conference on Magnetism and Magnetic MaterialsMMM2021](#), [65th Annual Conference on Magnetism and Magnetic MaterialsMMM2021](#), [65th Annual Conference on Magnetism and Magnetic MaterialsMMM2021](#), [65th Annual Conference on Magnetism and Magnetic MaterialsMMM2021](#), [65th Annual Conference on Magnetism and Magnetic MaterialsMMM2021](#) and [65th Annual Conference on Magnetism and Magnetic MaterialsMMM2021](#)

 This paper was selected as Featured



View Online



Export Citation



CrossMark

ARTICLES YOU MAY BE INTERESTED IN

[Semiconductor nanocrystal photocatalysis for the production of solar fuels](#)

The Journal of Chemical Physics **154**, 030901 (2021); <https://doi.org/10.1063/5.0032172>

[Evidence of phonon pumping by magnonic spin currents](#)

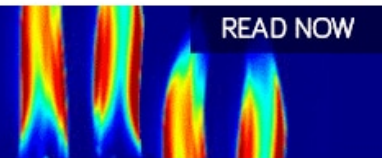
Applied Physics Letters **118**, 022409 (2021); <https://doi.org/10.1063/5.0035690>

[Laser-plasma acceleration beyond wave breaking](#)

Physics of Plasmas **28**, 013109 (2021); <https://doi.org/10.1063/5.0036627>

AIP Advances
Fluids and Plasmas Collection

READ NOW



Surface acoustic waves increase magnetic domain wall velocity

Cite as: AIP Advances 11, 015234 (2021); doi: 10.1063/9.0000159
 Presented: 6 November 2020 • Submitted: 22 October 2020 •
 Accepted: 4 December 2020 • Published Online: 15 January 2021



A. Adhikari^{a)} and S. Adenwalla

AFFILIATIONS

Department of Physics and Astronomy and Nebraska Center for Materials and Nanoscience, University of Nebraska-Lincoln, Lincoln, Nebraska 68588, USA

Note: This paper was presented at the 65th Annual Conference on Magnetism and Magnetic Materials.

^{a)}Author to whom correspondence should be addressed: aadhikari@huskers.unl.edu

ABSTRACT

Domain walls in magnetic thin films are being explored for memory applications and the speed at which they move has acquired increasing importance. Magnetic fields and currents have been shown to drive domain walls with speeds exceeding 500 m/s. We investigate another approach to increase domain wall velocities, using high frequency surface acoustic waves to create standing strain waves in a 3 micron wide strip of magnetic film with perpendicular anisotropy. Our measurements, at a resonant frequency of 248.8 MHz, indicate that domain wall velocities increase substantially, even at relatively low applied voltages. Our findings suggest that the strain wave derived effective magnetic field acts as an additional driver for domain wall motion.

© 2021 Author(s). All article content, except where otherwise noted, is licensed under a Creative Commons Attribution (CC BY) license (<http://creativecommons.org/licenses/by/4.0/>). <https://doi.org/10.1063/9.0000159>

The growing promise of racetrack memory technology¹ has led to an explosion in the investigation of the motion of domain walls (DW) in magnetic nanostructures. Defect free thin films, higher fields, and current²⁻⁴ have all been shown to increase DW velocities, but the latter two approaches increase overall power requirements, an undesirable trait.

Here we show that strain in the form of high frequency surface acoustic waves (SAW) result in a substantial increase in the DW velocity in a 3 μm wide magnetic stripe of a [Co/Pt]₅ multilayer with perpendicular magnetic anisotropy. The stripe is parallel to the propagation direction of the SAW and lies between two identical interdigital transducers (IDT) each with 100 finger pairs, all patterned via photolithography on a 128° Y cut LiNbO₃ substrate. The two IDTs are spaced an integer number of wavelengths apart and excited in parallel, generating a standing wave between them. Figures 1a and 1b show the geometry and coordinate system, the sample structure and the SAW wavelength. The frequency response of the reflection and transmission parameters, shown in Figures 1c and 1d, are measured using a spectrum analyzer (Agilent E7402A) and a bi-directional coupler (Mini-Circuit ZFBDC20-62HP+). The response of all four S-parameters over the frequency range 240-260 MHz

are measured to obtain the SAW resonance frequency (f_0) of 248.8 MHz.

The interaction between strain and magnetism is encompassed in the magneto-elastic constants and the free energy terms associated with them viz.

$$F_{ME} = B_1 (e_{xx}\alpha_{xx}^2 + e_{yy}\alpha_{yy}^2 + e_{zz}\alpha_{zz}^2) + B_2 (e_{xy}\alpha_x\alpha_y + e_{xz}\alpha_x\alpha_z + e_{yz}\alpha_z\alpha_y) \quad (1)$$

where B_1 and B_2 are the longitudinal and shear magneto-elastic constants which are material dependent, e_{ii} and e_{ij} constitute the longitudinal and shear strains in the magnetic film and the α_i are the direction cosines of the magnetization. The directions x, y, and z are as defined in Figures 1a and 1b, with the z axis perpendicular to the plane of the sample and the x axis parallel to the propagation direction of the SAW.

Previous experiments that explore the coupling between strain and magnetism include SAW driven magnetization rotation in cobalt microstructures⁵ and a lowered coercivity in in-plane Galfenol (FeGa) films⁶ and out of plane (Ga,Mn)(As,P).⁷ High frequency SAW driven magnetic resonances in Ni films⁸ and (Ga,Mn)(As,P)⁹ show that the direction of magnetization can be

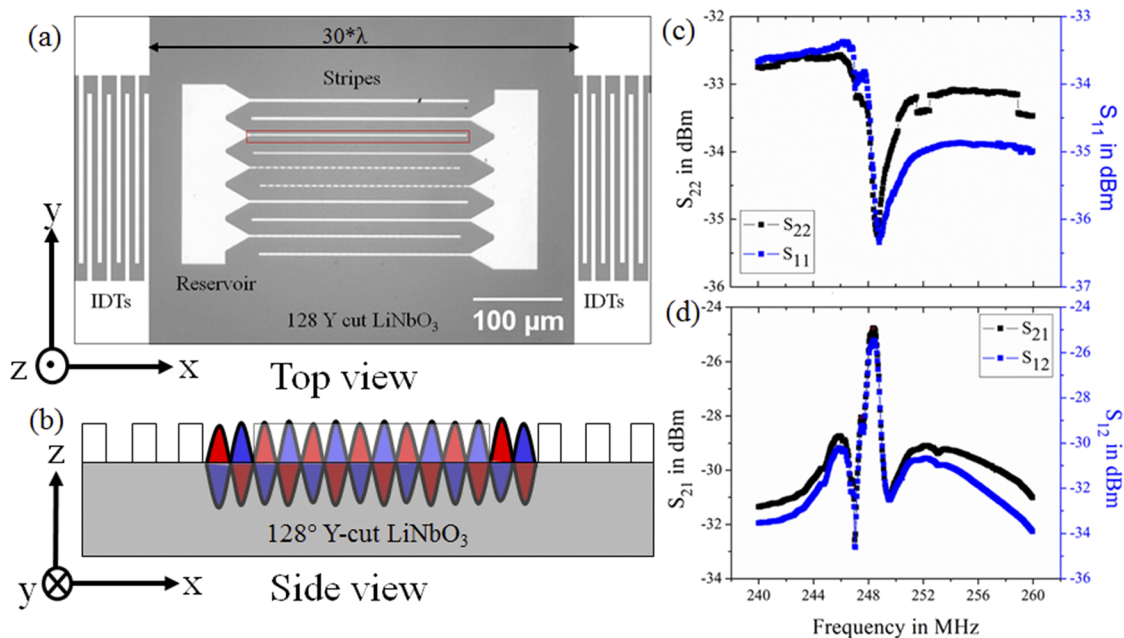


FIG. 1. (a) Schematic of the sample geometry in the x - y plane (top view). The sample consists of photolithographically patterned $\text{Cr}(2\text{nm})\text{Pt}(2\text{nm})[\text{Co}(0.4\text{nm})/\text{Pt}(0.6\text{nm})]_5/\text{Pt}(1\text{nm})$ (white area) on a 128° Y cut LiNbO_3 substrate (grey). The red rectangle indicates the $3\text{-}\mu\text{m}$ stripe on which all the measurements were performed. (b) Schematic (x - z plane) of the IDTs and standing waves when both IDTs are excited simultaneously and in phase. The frequency response of the (c) reflection parameters S_{11} and S_{22} and (d) transmission parameters S_{21} and S_{12} of the IDTs measured using a spectrum analyzer. Both indicate a resonance frequency of $f_0 = 248.8$ MHz.

reversed with appropriate control of the SAW pulse width. Our previous paper¹⁰ had shown that SAW were efficient drivers of DWs in a large area thin film. In this manuscript, we make detailed and wide-ranging measurements of the effects of SAW on DW velocity in a microscopic strip that restricts the direction of DW motion and allows us to quantitatively model the effects of the SAW.

Measurements of the DW velocity are made using a MOKE microscope and a pulsed magnetic field. The velocity measurements with SAW are performed using pulsed magnetic fields in the presence of a continuously driven SAW at the resonance frequency. The stripe is first saturated at a field of -750 Oe, followed by a nucleation field of 177 Oe. The DW nucleates in the reservoir close to the left end of the stripe and successive field pulses expand the domain along the stripe. We perform more than 10 measurements for each field to obtain the average velocity and standard error. Typical MOKE images of DW motion are shown in Figure 2. The motion of the DW in the absence of SAW is shown in Figure 2(a) with 20 ms field pulses of 142 Oe. Successive 20 ms pulses move the DW from left to right through the length of the magnetic stripe and the velocity is obtained by measuring the position of the domain wall after every pulse. A good measure of the increase in DW velocity can be seen in the number of pulses it takes to move the DW through the length of the stripe. In the absence of SAW, it takes ninety-seven 20-ms long pulses to move the DW across the stripe. In contrast, in the presence of a continuous SAW excitation of 4 V, (Figure 2b) the DW moves across the stripe in only sixteen pulses. This factor of

6 decrease in the number of pulses implies a 6-fold increase in the velocity. Videos of the DW propagation along the stripe at a field of 142 Oe with SAW excitations of 0 V, 2 V and 4 V are presented in supplementary material videos S1, S2 and S3, respectively.

We repeat the set of measurements at field values ranging from 118 to 190 Oe, and with SAW excitations ranging from 0 to 4 V. The velocity as a function of field with no SAW is shown in Figure 3(a) and displays the expected increase in velocity with increasing field. A plot of $\ln(v)$ vs $H^{-1/4}$ in the inset displays the linear dependence that would be expected in the creep regime^{11,12} i.e.,

$$V = V_o e^{-\frac{U_c}{k_B T} \left(\frac{H_{dep}}{H}\right)^\mu} \quad (2)$$

Here, v_o is a scaling parameter, U_c is the depinning potential, H_{dep} is the depinning field at 0 K and $\mu=1/4$ is the critical exponent. We extract the scaling parameter $\ln[v_o \text{ in } \mu\text{m/s}] = 62.0 \pm 0.9$ and depinning parameter, $\frac{U_c}{k_B T} (H_{dep})^{1/4} = 201.3 \pm 3.1 (\text{Oe})^{1/4}$ from the fit of the straight line in the inset. These numbers (derived for zero SAW excitation) characterize the average, overall pinning landscape seen by the DWs and we use them for fitting the SAW data. Experiments measuring the effects of DC strain on creep behavior have shown¹² that strain does not alter these parameters in any substantial fashion.

DW velocity data as a function of increasing SAW amplitudes are shown in Figure 3(b) for a range of field values, indicating a substantial increase in the DW velocity as a function of applied voltage

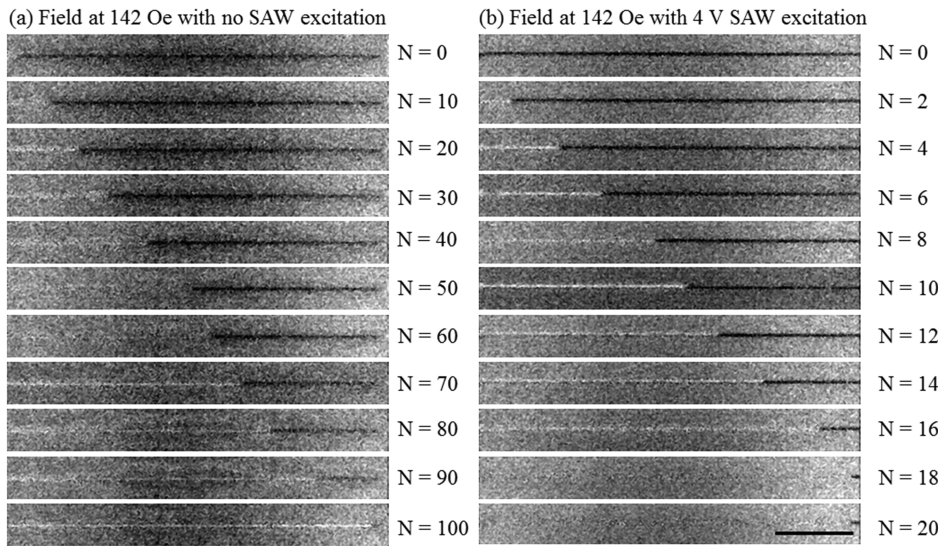


FIG. 2. MOKE images showing the domain wall moving from left to right along the stripe. N represents the number of magnetic field pulses. The scale bar on the lower right is $50 \mu\text{m}$ long. The field is applied in 20 ms pulses with an amplitude of 142 Oe (a) without SAW showing the motion of the DW after every 10 pulses and (b) with 4 V SAW excitation at the resonance frequency of 248.8 MHz showing the motion of the domain wall after every other pulse. A quick visual comparison shows that it only takes about 16 pulses with a 4 V SAW excitation to move the DW as far as 90 field pulses without SAW.

to the SAW. A comparison between Figures 3a and 3b shows that at a field value of 142 Oe , the DW velocity increases from 118 to $676 \mu\text{m/s}$ (nearly 6 times) at a SAW voltage of 4 V , as would be expected from the images in Figure 2b. Overall, a 3 - 8 fold increase in DW velocity with SAW excitations of 4 V are clearly visible.

The $\ln(v)$ vs $H^{-1/4}$ plot in Figure 4a for each SAW voltage shows sets of parallel lines, indicating that we remain in the creep regime. We model the effect of the SAW as an additional field and insert this effective field into the creep equation to fit the increased SAW driven velocity.

We start by simplifying the magneto-elastic terms in the free energy (Eq. (1)) for 128° Y cut LiNbO_3 and the magnetization of the sample. The out-of-plane anisotropy of the film ensures that $\alpha_x=0$ everywhere except at DWs. Moreover, if we assume a Néel DW

(as is commonly accepted) $\alpha_y = 0$ everywhere. Because the surface is stress free, the e_{zz} term arises only from the effective Poisson ratio for a $[\text{Co}/\text{Pt}]$ layer on LiNbO_3 , calculated to be¹³ $v_{\text{eff}} = -0.4$. Previous calculations¹⁰ indicate that propagation along the x axis in 128° Y cut LiNbO_3 results in shear strains that are substantially (>20 times) lower than e_{xx} . Hence the magneto elastic term in the free energy with the spatial and time dependence of the standing wave, may be approximated as

$$F_{ME} \approx B_1 (e_{xx} \alpha_{xx}^2 - 0.4 e_{xx} \alpha_{zz}^2) = B_1 (e_{00} V \alpha_{xx}^2 - 0.4 e_{00} V \alpha_{zz}^2) 2 \cos(kx) \cos(\omega t) \quad (3)$$

where e_{00} is the strain amplitude per unit voltage. Simulations have shown¹⁴ that the strain gradient is the leading driving term

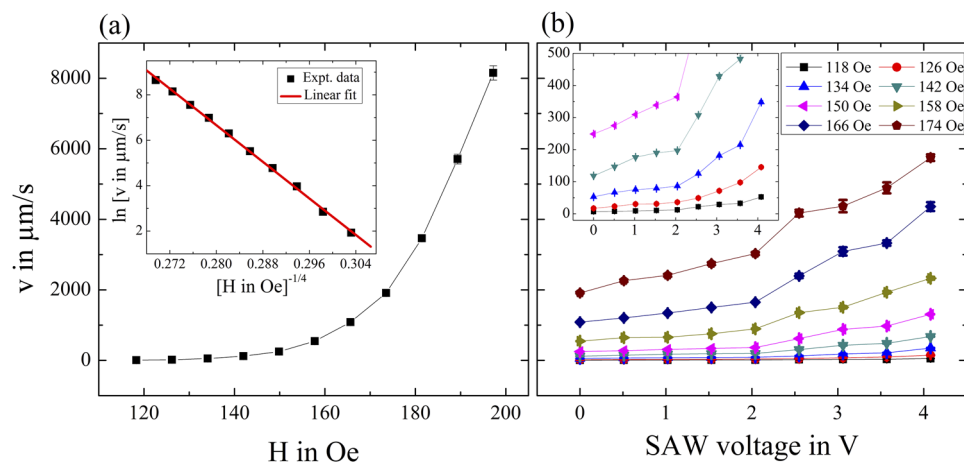


FIG. 3. (a) Average domain wall velocity for different fields. The error bar in the data is the standard error of 10 repeated measurements. Inset: the plot of $\ln[v]$ versus $(H)^{-1/4}$ of the same data. The red solid line is a linear fit. (b) Average domain wall velocity as a function of SAW excitation voltage at different field values. The inset shows a magnified view of the low field data. All lines are guides to the eye.

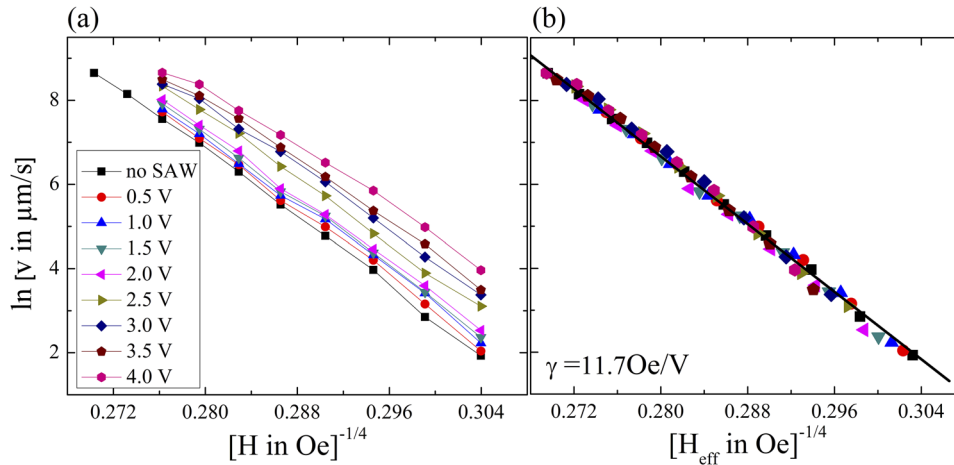


FIG. 4. (a) The plot of $\ln[v]$ versus $(H)^{-1/4}$ for different SAW voltages. (b) All data in (a) collapse to a single curve by defining $H \rightarrow H_{\text{eff}} = [(H_{\text{app}} + \beta\gamma V)^2 + (\gamma V)^2]^{1/2}$ in the creep equation, where β and γ are the only two fitting parameters. The black solid line is the linear fit with no SAW, (identical to that in the inset of Fig. 3(a)).

for DWs, implying that DWs will be driven most strongly at the nodes of the standing wave. Our data do not show any spatial dependence, perhaps due to the fairly low resonance frequency, which will limit the magnitude of the strain gradient. Moreover, because we are in the creep regime, the velocity changes we see are driven by the ability of DWs to depin from the pinning potential landscape.

The amplitude of the strain derived effective field is a derivative of the magneto-strictive free energy F_{ME} and is given by

$$\begin{aligned} H_{i(\text{SAW})} &= \frac{\partial F_{ME}}{\partial M_i} \rightarrow H_{x(\text{SAW})} \\ &= \frac{2B_1 e_{00} \alpha_x}{M_s} V \text{ and } H_{z(\text{SAW})} = -\frac{2(0.4)B_1 e_{00} \alpha_z}{M_s} V \end{aligned} \quad (4)$$

An absolute measure of this field is difficult to obtain because the conversion between voltage and strain field, the exact value for B_1 and direction of magnetization (α_x, α_z) inside the domain wall are subject to some uncertainty. However, we can assume that the strain is proportional to applied voltage. Both in-plane and out of plane fields are relevant to the depinning as has been shown in previous measurements.¹⁵ The ratio of H_z/H_x depends on α_x and α_z which vary across the DW, but we can assume that both are non-zero and both are proportional to V , so that the direction of the SAW induced field is somewhere in the x - z plane. Hence the net effective field for domain wall motion is given by the vector addition of the applied field (H_{app} in the z direction) and the SAW derived field (H_{SAW}), viz.

$$\vec{H}_{\text{eff}} = \vec{H}_{\text{app}} + \vec{H}_{\text{SAW}} = [(H_{\text{app}} + \beta\gamma V)^2 + (\gamma V)^2]^{1/2} \quad (5)$$

where $\gamma = \frac{2B_1 e_{00} \alpha_x}{M_s}$ encompasses the magneto-elastic constant, α_x and the conversion between applied voltage and strain amplitude and

$\beta = H_z/H_x$ accounts for the direction of H_{SAW} . The entire set of velocity data is modelled using β and γ as free parameters and the previously obtained v_0 and $\frac{U_c}{k_B T} (H_{\text{dep}})^{1/4}$ from the data without SAW excitation. Figure 4(b) shows that the entire data set collapses onto a single curve, that of the $V = 0$ line, with the best fit ($\chi^2 = 1.24$) obtained for values of $\beta = 0.2$ and $\gamma = 11.7 \text{ Oe/V}$. The small value for β implies an effective field close to the x axis direction. The total effective field per unit voltage produced by this particular set of SAW transducers $H_{\text{SAW}} = \sqrt{(H_x)^2 + (H_z)^2} = \gamma \sqrt{1 + \beta^2} = 11.9 \text{ Oe/V}$.

In summary, we have investigated the effects of SAW on domain wall velocities in multilayers of $[\text{CoPt}]_5$ over a wide range of field and SAW excitations. Domain wall velocities shows a dramatic 3-8 fold increase with SAW voltage. Modelling the SAW as an effective field collapses all the SAW data onto a single curve in the creep regime, manifesting the effectiveness of our model. The coupling parameter between SAW voltage and field is found to be 11.9 Oe/V , for this particular set of IDTs. Increasing the number of fingers and better impedance matching will contribute to higher SAW derived effective fields and hence higher DW velocities.

See [supplementary material](#) videos S1, S2 and S3 for domain wall propagation along the stripe at a field of 142 Oe and SAW voltages of 0V, 2V, and 4V, respectively.

This work was supported by NSF (DMR-1409622) and NSF Nebraska MRSEC (DMR-1420645). The research was performed in part in the Nebraska Nanoscale Facility: National Nanotechnology Coordinated Infrastructure and the Nebraska Center for Materials and Nanoscience, which are supported by the National Science Foundation under Award ECCS: 1542182, and the Nebraska Research Initiative.

DATA AVAILABILITY

The data that support the findings of this study are available from the corresponding author upon reasonable request.

REFERENCES

- ¹S.-H. Yang, K.-S. Ryu, and S. Parkin, "Domain-wall velocities of up to 750 m s^{-1} driven by exchange-coupling torque in synthetic antiferromagnets," *Nat. Nanotechnol.* **10**(3), 221–226 (2015).
- ²D. Atkinson, D. A. Allwood, G. Xiong, M. D. Cooke, C. C. Faulkner, and R. P. Cowburn, "Magnetic domain-wall dynamics in a submicrometre ferromagnetic structure," *Nat. Mater.* **2**(2), 85–87 (2003).
- ³M. Hayashi, L. Thomas, R. Moriya, C. Rettner, and S. S. P. Parkin, "Current-controlled magnetic domain-wall nanowire shift register," *Science* **320**(5873), 209–211 (2008).
- ⁴S. Emori, D. C. Bono, and G. S. D. Beach, "Time-resolved measurements of field-driven domain wall motion in a submicron strip with perpendicular magnetic anisotropy," *J. Appl. Phys.* **111**(7), 07D304 (2012).
- ⁵S. Davis, A. Baruth, and S. Adenwalla, "Magnetization dynamics triggered by surface acoustic waves," *Appl. Phys. Lett.* **97**(23), 232507 (2010).
- ⁶W. Li, B. Buford, A. Jander, and P. Dhagat, "Acoustically assisted magnetic recording: A new paradigm in magnetic data storage," *IEEE Trans. Magn.* **50**(3), 37–40 (2014).
- ⁷L. Thevenard *et al.*, "Strong reduction of the coercivity by a surface acoustic wave in an out-of-plane magnetized epilayer," *Phys. Rev. B* **93**(14), 140405 (2016).
- ⁸M. Weiler *et al.*, "Elastically driven ferromagnetic resonance in nickel thin films," *Phys. Rev. Lett.* **106**(11), 117601 (2011).
- ⁹L. Thevenard *et al.*, "Surface-acoustic-wave-driven ferromagnetic resonance in (Ga,Mn)(As,P) epilayers," *Phys. Rev. B: Condens. Matter Mater. Phys.* **90**(9), 094401 (2014).
- ¹⁰W. Edrington, U. Singh, M. A. Dominguez, J. R. Alexander, R. Nepal, and S. Adenwalla, "SAW assisted domain wall motion in Co/Pt multilayers," *Appl. Phys. Lett.* **112**(5), 052402 (2018).
- ¹¹P. J. Metaxas *et al.*, "Creep and flow regimes of magnetic domain-wall motion in ultrathin Pt/Co/Pt films with perpendicular anisotropy," *Phys. Rev. Lett.* **99**(21), 217208 (2007).
- ¹²P. M. Shepley, A. W. Rushforth, M. Wang, G. Burnell, and T. A. Moore, "Modification of perpendicular magnetic anisotropy and domain wall velocity in Pt/Co/Pt by voltage-induced strain," *Sci. Rep.* **5**, 7921 (2015).
- ¹³P. Manchanda, U. Singh, S. Adenwalla, A. Kashyap, and R. Skomski, "Strain and stress in magnetoelastic Co-Pt multilayers," *IEEE Trans. Magn.* **50**(11), 2504804 (2014).
- ¹⁴J. Dean, M. T. Bryan, J. D. Cooper, A. Virbule, J. E. Cunningham, and T. J. Hayward, "A sound idea: Manipulating domain walls in magnetic nanowires using surface acoustic waves," *Appl. Phys. Lett.* **107**(14), 142405 (2015).
- ¹⁵J. J. W. Goertz, G. Ziemys, I. Eichwald, M. Becherer, H. J. M. Swagten, and S. B.-V. Gamm, "Domain wall depinning from notches using combined in- and out-of-plane magnetic fields," *AIP Adv.* **6**(5), 056407 (2016).